Bioorganic & Medicinal Chemistry Letters 20 (2010) 2950–2953

Contents lists available at ScienceDirect

Bioorganic & Medicinal Chemistry Letters

journal homepage: www.elsevier.com/locate/bmcl

Molecular modelling, synthesis and acetylcholinesterase inhibition of ethyl 5-amino-2-methyl-6,7,8,9-tetrahydrobenzo[*b*][1,8]naphthyridine-3-carboxylate

Elena Soriano [a], Abdelouahid Samadi [a], Mourad Chioua [a], Cristóbal de los Ríos [b], José Marco-Contelles [a,*]

[a] *Laboratorio de Radicales Libres y Química Computacional (LRL-QC, IQOG, CSIC), C/Juan de la Cierva 3, 28006-Madrid, Spain*
[b] *Departamento de Farmacología y Terapéutica, Facultad de Medicina, Universidad Autónoma de Madrid, C/Arzobispo Morcillo 4, 28029 Madrid, Spain*

ARTICLE INFO

Article history:
Received 30 December 2009
Revised 27 February 2010
Accepted 2 March 2010
Available online 4 March 2010

Keywords:
Molecular modelling
Ethyl 5-amino-2-methyl-6,7,8,9-tetrahydrobenzo[*b*][1,8]naphthyridine-3-carboxylate
AChE/BuChE inhibition
Alzheimer's disease

ABSTRACT

In silico analysis of ethyl 5-amino-2-methyl-6,7,8,9-tetrahydrobenzo[*b*][1,8]naphthyridine-3-carboxylate (**2**) predicts that this molecule should be successfully docked in the PAS, and easily accommodated in the CAS of AChE. The synthesis and the AChE/BuChE inhibition studies are reported, confirming that compound **2** is a potent and selective AChE inhibitor, and consequently, a new lead compound for further development into new dual CAS/PAS cholinergic agents for the treatment of Alzheimer's disease.

Alzheimer's disease (AD)[1] is a pathology where diverse factors, such as amyloid-β, deposits in senile plaques,[2] τ-protein aggregation,[3] oxidative stress and low levels of acetylcholine[4] are thought to play significant roles.[5] The cholinergic hypothesis,[6] the most successful approach for the symptomatic treatment of AD, postulates that at least some of the cognitive decline results from a deficiency in acetylcholine and thus in cholinergic neurotransmission. Therefore, inhibition of acetylcholinesterase (AChE) appears to be a strategy to reduce the cognitive deficit in AD. To this end some AChE inhibitors have been developed for the symptomatic treatment of AD, such as those reported by Renard,[7] Barreiro,[8] Hu,[9] Desai,[10] and others.[11] In this context, we have reported the synthesis and the AChE/BuChE inhibitory activity of a series of tacrine analogues (**A** and **B**, Chart 1), where the benzene ring has been substituted by a 4*H*-pyran, a pyridine or a 1,4-DHP ring system, and the cyclohexyl ring has been contracted or enlarged to a cyclopentyl or a cycloheptyl, respectively.[12] The results revealed that the substitution of a benzene ring in the tacrine core by 4*H*-pyran or pyridine rings generates mixed and potent AChE/BuChE inhibitors, but less active than tacrine, the benzo[*b*][1,8]naphthyridines (i.e., bearing an aromatic ring at C4) being the most active in this series.[12] Molecular modelling results on compound **1** (Chart 1) suggested that the binding to the AChE catalytic active site (CAS) might be hampered by unfavourable steric interactions due to the aromatic substituent at C-4.[12] As a result, the pass through the gorge to reach the CAS might be difficult, resulting in a displacement of inhibitor **1** to the peripheral anionic site (PAS). Therefore, it could be of interest to explore new inhibitors able to bind at both catalytic and peripheral binding sites of AChE, and on the basis of these previous findings, we hypothesized that structure **2** (Chart 1), lacking of the aromatic ring at C4, could be easily accommodated in the AChE active site, besides in the PAS of AChE. Accordingly, in this Letter we describe the molecular modelling of compound **2** showing that this molecule is successfully docked in the PAS, and easily accommodated in the CAS of AChE; next, to confirm this hypothesis we have carried out the synthesis, and the AChE/BuChE inhibition of the new tacrine derivative **2**.

A molecular modelling study was performed to determine the binding mode of this inhibitor to the AChE as described in Methods in the Supplementary data. Firstly, a docking analysis was performed with AutoDock program. A box encompassing both the CAS and the PAS was defined for the exploration of possible binding modes. The results showed that the ligand was exclusively docked at the CAS. In a second round of docking experiments, we built smaller grids around both potential binding sites. Under these conditions, we found two different binding modes at the CAS and one more at the PAS. At the latter, that is at the mouth of the gorge, the [1,8]naphthyridine core shows π–π stacking interactions with the residues Trp286 and Tyr341, whereas the amino group and the carboxylic ester can establish a hydrogen bond with the side chains of Asp74 and Tyr72, respectively (see Fig. 1). In this

* Corresponding author. Tel.: +34 91 5622900; fax: +34 91 5644853.
E-mail address: iqoc21@iqog.csic.es (J. Marco-Contelles).

0960-894X/$ - see front matter © 2010 Elsevier Ltd. All rights reserved.
doi:10.1016/j.bmcl.2010.03.010

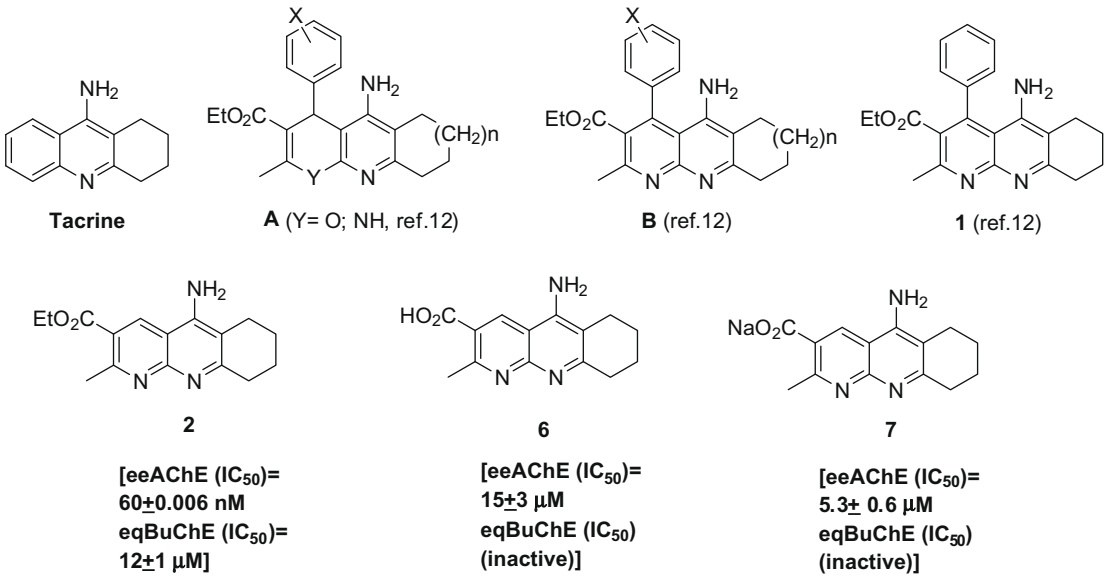

Chart 1. Tacrine analogues and AChE/BuChE inhibition values.

orientation, the cycloalkene unit is buried inside the protein gorge and does not make favourable contacts, but lies close to the side chain of Phe338 and Phe297. At the CAS the two binding modes **IIa** and **IIb** proposed by the docking study are as follows (see Fig. 1): (i) In the complex **IIa**, the [1,8]naphthyridine scaffold is stacked against the aromatic rings of Trp86 and Tyr337. The aromatic nitrogen at the central ring, protonated at the physiological pH, is hydrogen-bonded to the backbone carbonyl oxygen of His447. This binding mode is analogous to that found in the crystallographic complex of tacrine bounded at the CAS of AChE from *Torpedo californica* (pdb code 1ACJ),[13,14] and (ii) alternatively, the binding pose for the complex **IIb** also involves the stacking interactions with Trp86 and Tyr337 but the amino substituent is doubly hydrogen bonded to the His447 backbone and side chain of Glu202. The biochemical role of this last residue in catalysis is well established,[15] but interaction with it has been barely exploited in the design of more potent tacrine-like reversible inhibitors. In this respect, it is worth recalling that the carboxylate of this Glu establishes a hydrogen bond with a hydroxyl group of the reversible AChE inhibitor galanthamine,[16] as well as a water-mediated hydrogen bond with the pyridine nitrogens of (−)-huperzine A.[17] Finally, the ester in complex **IIb**, occupies a hydrophobic pocket formed by Trp439, Met443 and Pro446. The use of this pocket has been identified for other inhibitors in both modelling studies and X-ray crystallographic structures of AChE-ligand complexes to account for an increased inhibitory potency (huprines X and Y).[18]

The position of **IIa** and **IIb** with respect to selected key residues in the binding site is shown in Figure 1. These results (see also Table 1 in the Supplementary data) suggest that this compound could be easily accommodated in the CAS of AChE. In order to verify this hypothesis and gain insights about the binding affinity and stability of **1** at the catalytic site, a series of 10 ns molecular dynamics (MD) simulations have been performed. As long as the preferred orientation of compound **2** in the CAS is a critical issue for designing novel dual inhibitors, both binding modes of **IIa** and **IIb** complexes has been explored. The temperature, the total energy, the mass density and the energy components of the system were inspected to evaluate the stability of the trajectory. The root-mean square deviation (RMSD) profiles from the protein X-ray structure have been monitored for the backbone and heavy atoms to get insights into the changes that are experienced upon binding (Fig. 2, Supplementary data). For **IIb**, the RMSD deviations determined for the backbone and heavy atoms rise smoothly and continuously along the simulation pointing to a low stability. For **IIa** they rise during the first nanosecond, but remained nearly constant for the rest of the trajectory, around 1.1 and 1.6 Å, respectively, which indicates a structural stability of the complex along the trajectory (Fig. 2, Supplementary data). A close inspection of the initial and averaged structures suggests that critical rearrangements that might account for the deviations for **IIb** are those induced by the ester moiety of the ligand, since it forces the side chains of residues on the hydrophobic pocket away (Figs. 3 and 4). The analysis of the intermolecular hydrogen bonds formed upon complexation has revealed that for **IIb** the hydrogen bonds to His447 and Glu202 were kept throughout the trajectory, with an average N···O distance of 3.03 and 2.98 Å, respectively. For **IIa** the hydrogen-bond of the aromatic nitrogen, protonated at the physiological pH, to the main chain carbonyl oxygen of His447 is stronger (average N···O distance of 2.89 Å), and occupied 100% throughout the simulation. The aromatic core is firmly stacked against the aromatic rings of Trp86 and Tyr337 for both binding modes (average distances from the central ring for **IIa** of 3.56 and 4.43 Å, and for **IIb** of 3.63 and 4.31 Å, respectively). The ester group was progressively rotated during the MD simulation until coplanarity with the aromatic scaffold, which hampers an effective H-bond with the closer H-bond donor residues. Moreover, for the complex **IIb** this conformational change induces unfavourable steric interactions with neighbouring residues at the hydrophobic pocket which forces a more intense distortion than for **IIa** to avoid steric clashes, as is supported by the RMSD profiles (Fig. 3).

Figure 5 shows a representation of both binding modes in average structures of the last 5 ns of the MD simulation. MM/PBSA (= Molecular Mechanics/Poisson Boltzmann Surface Area) calculations, performed for the snapshots collected along the last 2 ns to examine the relative stabilities, reveal that the binding mode for the complex **IIa** is favored by 8.3 kcal mol^{-1} over **IIb**. This is due to a larger internal destabilization for **IIb** which agrees with the structural distortion observed in the RMDS profiles. Indeed, the residues in the CAS (particularly, in the hydrophobic pocket) show rearrangement to accommodate the ligand (Figs. 3 and 4). In summary, the calculations suggest that the ligand is successfully docked in the PAS and that it can be easily accommodated in the CAS to form the complex **IIa** which shows a high stability, as supported by MD computations.

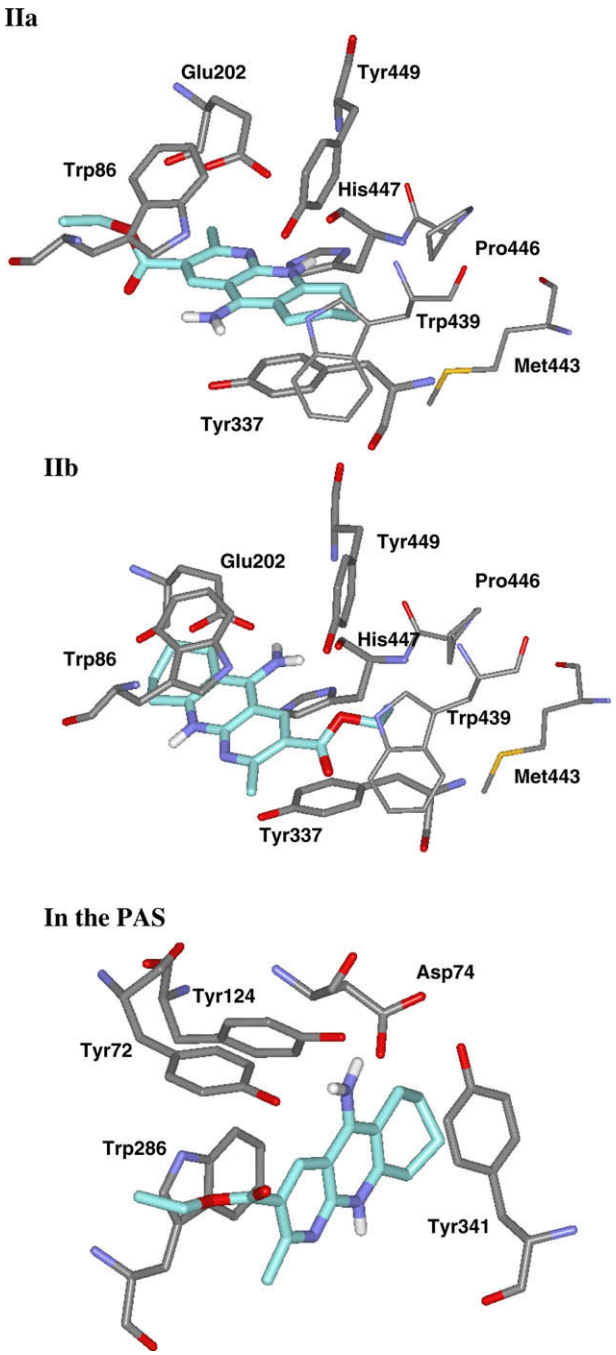

Figure 1. Representation of the binding modes **IIa** and **IIb** in the CAS and in the PAS predicted by the docking study. Relevant residues are shown as sticks and coloured by atoms (C, grey). The residues forming the hydrophobic pocket (Trp439, Met443, Pro446) are depicted as thin sticks. Ligand **1** is coloured by atoms (C, cyan).

Based on the interesting results, and in order to prove this hypothesis, we have synthesized compound **2**, as shown in Scheme 1. The reaction of commercially available ethyl ester of β-amino-crotonic acid (**3**) with 2-(ethoxymethylene)malononitrile (**4**) provided 2-amino-3-cyano-5-ethoxycarbonyl-6-methylpyridine **5**[19a–c] in 22% yield (not optimized), whose Friedländer reaction[20] with cyclohexanone, under $AlCl_3$ catalyzed and promoted microwave irradiation, afforded compound **2** in 30 min, and 90% chemical yield (see Supplementary data).

The biological evaluation of compound **2** has been carried out on eeAChE/hAChE, and eqBuChE, according to the usual protocols.[12] As

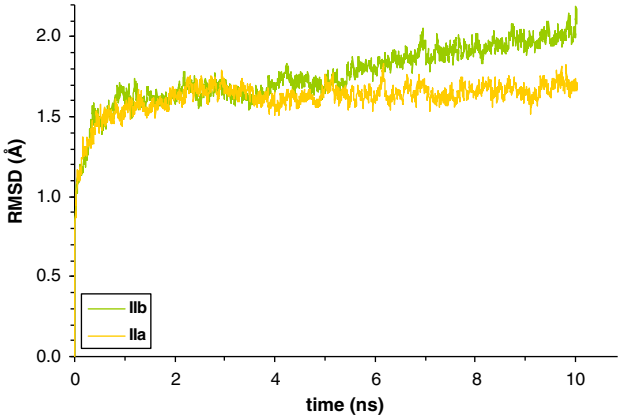

Figure 3. Time dependence of the positional root-mean square deviation (RMSD; Å) of the heavy atoms in the binding site for the AChE complexes **IIa** and **IIb**. For **IIb**, a continuous increasing is observed.

shown in Chart 1, compound **2** [eeAChE (IC_{50}) = 60 ± 0.006 nM; hAChE (IC_{50}) = 780 ± 0.08 nM] is a potent, in the nanomolar range, and selective AChE inhibitor versus BuChE [eqBuChE (IC_{50}) = 12 ± 1 μM], confirming the predictions of the molecular modelling. Compared with compound **1** [eeAChE (IC_{50}) = 822 nM; eqBuChE (IC_{50}) = 5.03 ± 0.57 μM][12] (Chart 1), **2** is a more potent inhibitor for AChE, but less potent for BuChE. Thus, it is clear that in going from compound **1** to **2**, by elimination of the aromatic ring at C4, the AChE potency is increased, while the BuChE inhibition is moderately lowered, promoting the binding at the CAS.

In summary, in this work we have investigated the molecular modelling of ethyl 5-amino-2-methyl-6,7,8,9-tetrahydrobenzo[*b*][1,8]naphthyridine-3-carboxylate (**2**), reported the synthesis and described its AChE/BuChE inhibition. We have shown that structure **2** can perfectly fit in the CAS (and PAS) of AChE. Consequently, the determination of the binding mode in the CAS should allow us a more successful design of novel dual AChE inhibitors. For instance, and as shown in Figure 5, based on binding mode **IIa**, we know now that the structural and functional motifs around the ethyl carboxylate moiety on compound **2**, point to the PAS, indicating thus the zone where we could make modifications to prepare new dual AChE inhibitors, such as dimers of compound **2** or heterodimers of compounds **1** and **2**, linking the monomers with

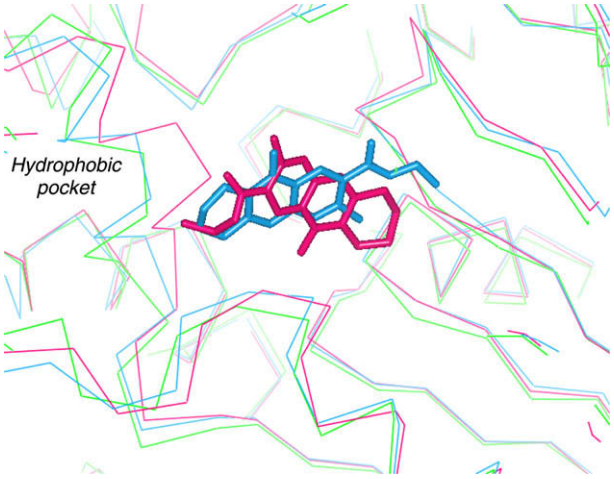

Figure 4. View of superimposed C(α) traces of the energy minimized average structure of the last 5 ns of the MD simulation of **IIa** (blue), **IIb** (magenta) and the initial X-ray structure (green). A larger deviation in the hydrophobic pocket is observed for **IIb**.

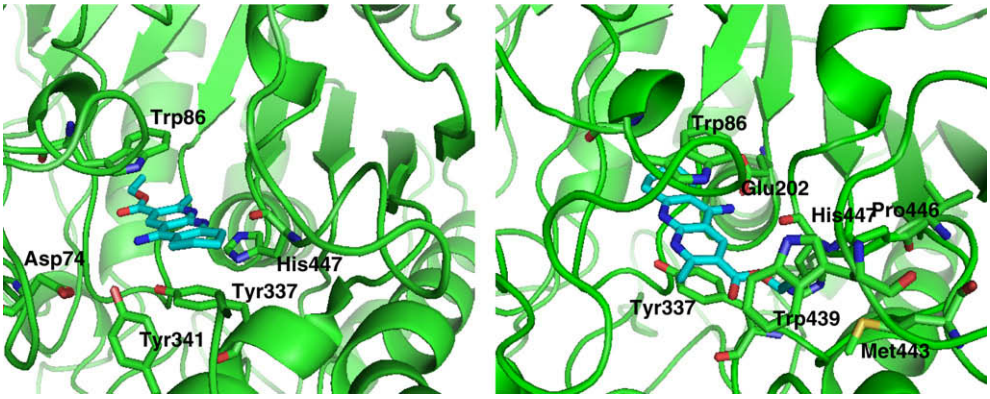

Figure 5. Schematic representation of the two binding modes from MD simulations: **IIa**, left; **IIb**, right. The C(α) traces of the enzyme is displayed as a ribbon. Some relevant residues are shown as sticks. Ligand is displayed as sticks with carbon atoms in cyan.

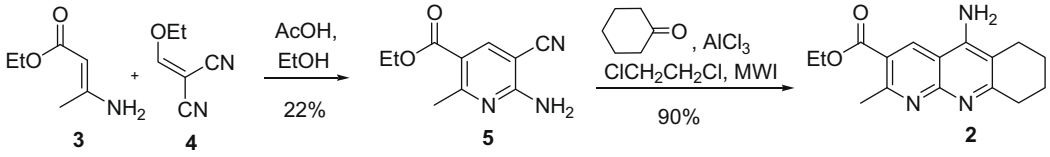

Scheme 1. Synthesis of ethyl 5-amino-2-methyl-6,7,8,9-tetrahydrobenzo[*b*][1,8]naphthyridine-3-carboxylate (**2**).

a suitable spacer, whose length and functionalities should be selected after molecular modelling. This chemistry, as well as the development of new derivatives of the lead-compound **2**, are obvious issues that should be addressed in our laboratory in a near future, and will be communicated in due course.[21]

Acknowledgements

Abdelouahid Samadi thanks CSIC for a I3P post-doctoral contract. Mourad Chioua thanks Instituto de Salud Carlos III (ISCIII, MICINN) for a 'Sara Borrell' contract. Elena Soriano and José Marco-Contelles (J.M.C.) thanks CSIC (200880I221), CAM-CSIC (CCG08-CSIC/SAL-3696) and Ministerio de Ciencia e Innovación (MICINN) (SAF2006-08764-C02-01), Comunidad Autónoma de Madrid (S/SAL-0275-2006) and ISCIII [Red RENEVAS (RD06/0026/1002)] for support. J.M.C. thanks Prof. Antonio García García and Dr. Mercedes Villarroya (Departamento de Farmacología y Terapéutica, Facultad de Medicina, Universidad Autónoma de Madrid, C/Arzobispo Morcillo 4; 28029 Madrid, Spain) for continuous support and encouragement.

Supplementary data

Supplementary data associated with this article can be found, in the online version, at doi:10.1016/j.bmcl.2010.03.010.

References and notes

1. Whitehouse, P. J.; Price, D. L.; Clark, A. W.; Coyle, J. T.; DeLong, M. R. *Ann. Neurol.* **1981**, *10*, 122.
2. Neve, R. L.; McPhie, D. L.; Chen, Y. *Brain Res.* **2000**, *886*, 54.
3. Crowther, R. A.; Goedert, M. J. *Struct. Biol.* **2000**, *130*, 271.
4. Cummings, J. L. *Rev. Neurol. Dis.* **2004**, *1*, 60.
5. Scarpini, E.; Scheltens, P.; Feldman, H. *Lancet Neurol.* **2003**, *2*, 539.
6. Bartus, R.; Dean, R.; Beer, B.; Lippa, A. *Science* **1982**, *217*, 408.
7. Ronco, C.; Sorin, G.; Nachon, F.; Foucault, F.; Jean, L.; Romieu, A.; Renard, P.-Y. *Bioorg. Med. Chem.* **2009**, *17*, 4523.
8. Barreiro, E. J.; Camara, C. A.; Verli, H.; Brazil-Más, L.; Castro, N. G.; Cintra, W. M.; Aracava, Y.; Rodrigues, C. R.; Fraga, C. A. M. J. *Med. Chem.* **2003**, *46*, 1144.
9. Hu, M.-K. J. *Pharm. Pharmacol.* **2001**, *53*, 83.
10. Desai, M. C. Patent Appl. U.S. 1993 520440.
11. León, R.; de los Ríos, C.; Marco-Contelles, J.; Huertas, O.; Barril, X.; Luque, F. J.; López, M. G.; García, A. G.; Villarroya, M. *Bioorg. Med. Chem.* **2008**, *16*, 7759.
12. Marco, J. L.; de los Ríos, C.; García, A. G.; Villarroya, M.; Carreiras, M. C.; Martins, C.; Eléuterio, A.; Morreale, A.; Orozco, M.; Luque, F. J. *Bioorg. Med. Chem.* **2004**, *12*, 2199.
13. Harel, M.; Schalk, I.; Ehret-Sabatier, L.; Bouet, F.; Goeldner, M.; Hirth, C.; Axelsen, P. H.; Silman, I.; Sussman, J. L. *Proc. Natl. Acad. Sci. U.S.A.* **1993**, *90*, 9031.
14. There are small structural changes at the catalytic binding site between *Tc*AChE and hAChE except for those of Tyr337 (in hAChE; Phe330 in *Torpedo californica* AChE, *Tc*AChE).
15. Wlodek, S. T.; Antosiewicz, J.; Briggs, J. M. J. *Am. Chem. Soc.* **1997**, *119*, 8159.
16. Bartolucci, C.; Perola, E.; Pilger, C.; Fels, G.; Lamba, D. *Proteins* **2001**, *42*, 182.
17. Raves, M. L.; Harel, M.; Pang, Y.-P.; Silman, I.; Kozikowski, A. P.; Sussman, J. L. *Nat. Struct. Biol.* **1997**, *4*, 57.
18. Camps, P.; El Achab, R.; Morral, J.; Muñoz-Torrero, D.; Badía, A.; Baños, J. E.; Vivas, N. M.; Barril, X.; Orozco, M.; Luque, F. J. J. *Med. Chem.* **2000**, *43*, 4657.
19. a Goldfarb, D. S. Patent Appl. U.S. 2009 163545.; (b) Yakovlev, M. Yu.; Romanova, O. B.; Grizik, S. I.; Kadushkin, A. V.; Granik, V. G. *Khimiko-Farmatsevticheskii Zhurnal* **1997**, *31*, 44; (c) Deyanov, A. B.; Niyazov, R. Kh.; Nazmetdinov, F. Ya.; Syropyatov, B. Ya.; Kolla, V. E.; Konshin, M. E. *Khimiko-Farmatsevticheskii Zhurnal* **1991**, *25*, 31; For a recently published synthesis of new aminonicotinate derivatives using a related protocol, see: (d) Ravinder, M.; Sadhu, P. S.; Santhoshi, A.; Narender, P.; Swamy, G. Y. S. K.; Ravikumar, K.; Rao, V. J. *Synthesis* **2010**, 573.
20. Marco-Contelles, J.; Pérez-Mayoral, M. E.; Samadi, A.; Carreiras, M. C.; Soriano, E. *Chem. Rev.* **2009**, *109*, 2652.
21. Based on a reviewer's suggestion, the free acid (**6**) (Chart 1) {mp >170 °C (dec); IR (KBr) *ν* 3368, 3067, 2953, 1684, 1630, 1599, 1541, 1490, 1406, 1368, 1356, 1265 cm^{-1}; ^1H NMR (500 MHz, CD_3OD-d_4) δ 8.72 (s, 1H, H4), 2.94 (m, 2H, 2H9), 2.84 (s, 3H, CH_3), 2.53 (m, 2H, 2H6), 1.95 (m, 4H, 2H7, 2H8); ^{13}C NMR (125 MHz, CD_3OD-d_4) δ 174.2 (C=O), 165.0 (C2), 158.4 (C5), 153.9 (C9a), 147.1 (C10a), 136.2 (C3), 132.0 (C4), 111.1 (C5a), 109.0 (C4a), 29.1 (C9), 24.7 ($CH_3C(2)$), 23.5 (C6), 22.5 (CH_2), 21.9 (CH_2); MS (ES) *m*/*z* (%): 258 $[M+H]^+$ (100). HRMS (ESI): Calcd for $C_{14}H_{15}N_3O_2$: 257.1164. Found: 257.1163. Anal. Calcd for $C_{14}H_{15}N_3O_2 \cdot 2/3H_2O$: C, 59.14; H, 6.38; N, 14.78. Found: C, 59.57; H, 6.21; N, 14.79}, or as its sodium salt (**7**) (Chart 1) {mp 267–269 °C; IR (KBr) *ν* 3074, 1687, 1617, 1413, 1371, 1242 cm^{-1}; ^1H NMR (500 MHz, DMSO-d_6) δ 9.26 (s, 1H, H4), 8.67 (s, 2H, NH_2), 2.89 (m, 2H, CH_2), 2.81 (s, 3H, CH_3), 2.48 (m, 2H, CH_2), 1.80 (m, 4H, 2CH_2); ^{13}C NMR (125 MHz, DMSO-d_6) δ 167.5 (CO), 163.4 (C2), 155.7 (C5), 153.9 (C9a), 147.2 (10a), 134.9 (C4), 128.2 (C3), 109.7 (C5a), 107.7 (C4a), 28.4 (CH_2), 24.8 (CH_3), 22.5 (CH_2), 21.0 (CH_2), 20.5 (CH_2); MS (ESI) *m*/*z* (%): $[M+1]^+$ 258.0, $[M+Na]^+$ 280.0; GC/MS (EI, 70 eV) *m*/*z* (%): 257 $[M^+]$, 100], 242 $[M^+-CH_3]$, 9], 241 $[M^+-NH_2]$, 11], 229 $[M^+-CO_2H]$, 8]. HRMS (ESI): Calcd for $C_{14}H_{15}N_3O_2$: 257.1164. Found: 257.1173. Anal. Calcd for $C_{14}H_{14}N_3O_2Na \cdot H_2O$: C, 56.56; H, 5.42; N, 14.13. Found: C, 56.21; H, 5.69; N, 14.35}, have been synthesized (the details will be further reported in a full paper), and their AChE/BuChE inhibition activities measured as usual. These data have been incorporated in Chart 1. Very interestingly, compounds **6** and **7** are less potent AChEI than ester **2**, and inactive for BuChE inhibition.